A Journal of the Gesellschaft Deutscher Chemiker

Angewandte International Edition Chemie

GDCh

www.angewandte.org

## Accepted Article

**Title:** Tetrazole-Based Probes for Integrated Phenotypic Screening, Affinity-Based Proteome Profiling and Sensitive Detection of a Cancer Biomarker

**Authors:** Zhengqiu Li, Ke Cheng, Jun-Seok Lee, Shao Q Yao, and Ke Ding



**To be cited as:** *Angew. Chem. Int. Ed.* 10.1002/anie.201709584
*Angew. Chem.* 10.1002/ange.201709584

**Link to VoR:** http://dx.doi.org/10.1002/anie.201709584
http://dx.doi.org/10.1002/ange.201709584

WILEY-VCH

10.1002/anie.201709584

**Target identification**

DOI: 10.1002/anie.200((will be filled in by the editorial staff))

# Tetrazole-Based Probes for Integrated Phenotypic Screening, Affinity-Based Proteome Profiling and Sensitive Detection of a Cancer Biomarker

*Ke Cheng, Jun-Seok Lee, Piliang Hao, Shao Q. Yao, Ke Ding* and Zhengqiu Li**

***Abstract**: Phenotypic screening has been a powerful approach in drug discovery, however it is hindered by difficulties in identifying the underlying cellular targets. To address this challenge, we have combined phenotypic screening of a fully functionalized small-molecule library with competitive affinity-based proteome profiling to map and functionally characterize the targets of screening hits. Using this approach, we identified ANXA2, PDIA3/4, FLAD1 and NOS2 as primary cellular targets of two bioactive molecules that inhibit cancer cell proliferation. We further demonstrated that a panel of probes can label and/or imagine annexin A2 (a cancer biomarker) from different cancer cell lines, thus providing opportunities for potential cancer diagnosis and therapy.*

Phenotypic screening plays a pivotal role in the discovery of novel bioactive compounds.[1] However, the utility of phenotypic screening is limited by its difficulties in identifying the underlying cellular targets.[2] Common approaches for target identication, such as in vitro-based assay and affinity chromatography, mostly rely on recombinant proteins or crude cell lysates, rendering them unsuitable for reporting genuine drug-protein interactions under native environments.[3] To address these challenges, affinity-based proteome profiling (A*f*BP), in which photoprobes capable of recapitulating drug-protein interactions *in situ* leading to subsequent protein enrichment and large-scale proteome-wide target identification, has been developed as a powerful approach for *in situ* target identification during the past decade.[4] In order to further improve this approach, we have developed three types of "minimalist" bioorthogonal handle-containing photo-crosslinkers (**L3-6**) capable of facilitating the synthesis of affinity-based probes (A*f*BPs) and enabling simultaneous proteome profiling and live-cell imaging.[5]

As a widely applied approach for target identification, A*f*BP still suffers from two key issues - nonspecific labeling and unsatisfactory photo-crosslinking yield.[6] To alleviate these issues, competitive proteome profiling is usually employed to distinguish between background labeling and specific crosslinking.[7] On the other hand, several groups have comprehensively studied the backgroun inventory of different photo-crosslinkers, which can help t eliminate nonspecifically labeled proteins from target candidates.[ Moreover, we have recently developed novel diaryltetrazole-base photo-crosslinkers, which possess superior photo-crosslinkin efficiency and one-/two-photon fluorescence turn-on properties, an are suitable for simultaneous in situ proteome profiling and no-was real-time imaging.[9] Owing to their unique crosslinking mechanisr (Figure 1A), the photo-induced nitrile imines generated from thes photo-crosslinkers are capable of undergoing rapid reactions with variety of biological nucleophiles (i.e. acids, thiols, amines, etc) an electrophiles (i.e. electron-deficient alkenes), but have show preferential labeling of proteins at their aspartic acid (Asp)/glutami acid (Glu) residues with reduced photo-crosslinker-associate nonspecific background labeling. Despite frequent occurrence in protein (> 12% with combined proportion of Asp and Glu),[10] fe carboxylate-selective protein labeling chemistries are currentl available.[11] Our findings were further confirmed by a follow-u work from Lin's group which showed 2-aryl-5-carboxytetrazol (ACT) can serve as an excellent photo-crosslinker in A*f*B studies.[12]

Recently, Cravatt et al. reported that phenotypic screening an target identification can be integrated by using affinity-based prob compound libraries, so as to accelerate the mechanisti characterization of screening hits.[13] Inspired by these elegar

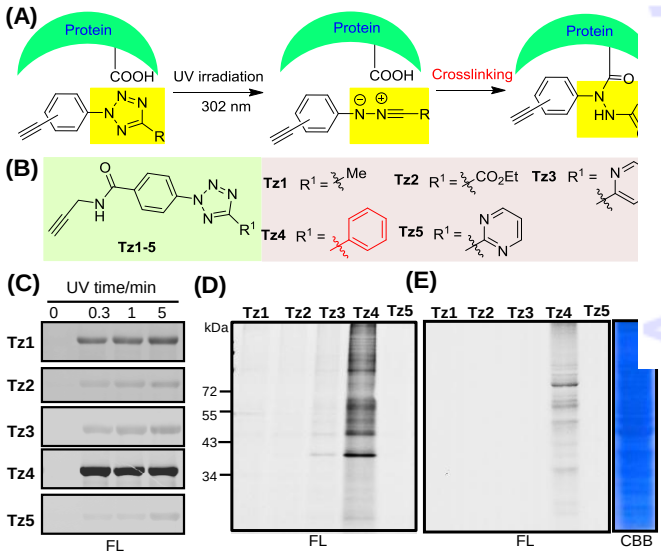


***Figure 1***. (A) The carboxylate-selective photo-crosslinking mechanism between a tetrazole and a protein. (B) Structures of compounds **Tz1-5**. (C) Time-dependent labeling of BSA (2 μg) with **Tz1-5** (1 μM) in PBS buffer. Proteome reactivity profiles of cell lysates (D) and live MCF-7 cells (E) treated with **Tz1-5**. FL = in-gel fluorescence scanning. CBB = Coomassie gel.

[1] K. Cheng, Prof. K. Ding, Prof. Z. Li
School of Pharmacy, Jinan University
601 Huangpu Avenue West, Guangzhou, China 510632
Email: pharmlzq@jnu.edu.cn, dingke@jnu.edu.cn
[2] Prof. Shao Q. Yao
Department of Chemistry, National University of Singapore
[3] Prof. J.-S. Lee
Molecular Recognition Research Center, Korea Institute of Science and Technology (KIST), and Department of Biological Chemistry, University of Science & Technology (Republic of Korea)
[4] Prof. P. Hao, School of Life Science and Technology, ShanghaiTech University, China

[**] Funding was provided by National Natural Science Foundation of China (21602079), Science and Technology Program of Guangdong province (2017A050506028), Science and Technology Program of Guangzhou (201704030060), KIST (2E26632/2E26110, CAP- 16-02-KIST) and the Bio & Medical Technology Development Program of the National Research Foundation (NRF- 2016M3A9B6902060) from Ministry of Science, Korea. We thank Dr. W. Lorenzo (JNU), Dr. L. Gao (IBN) for the invaluable suggestions on this work.

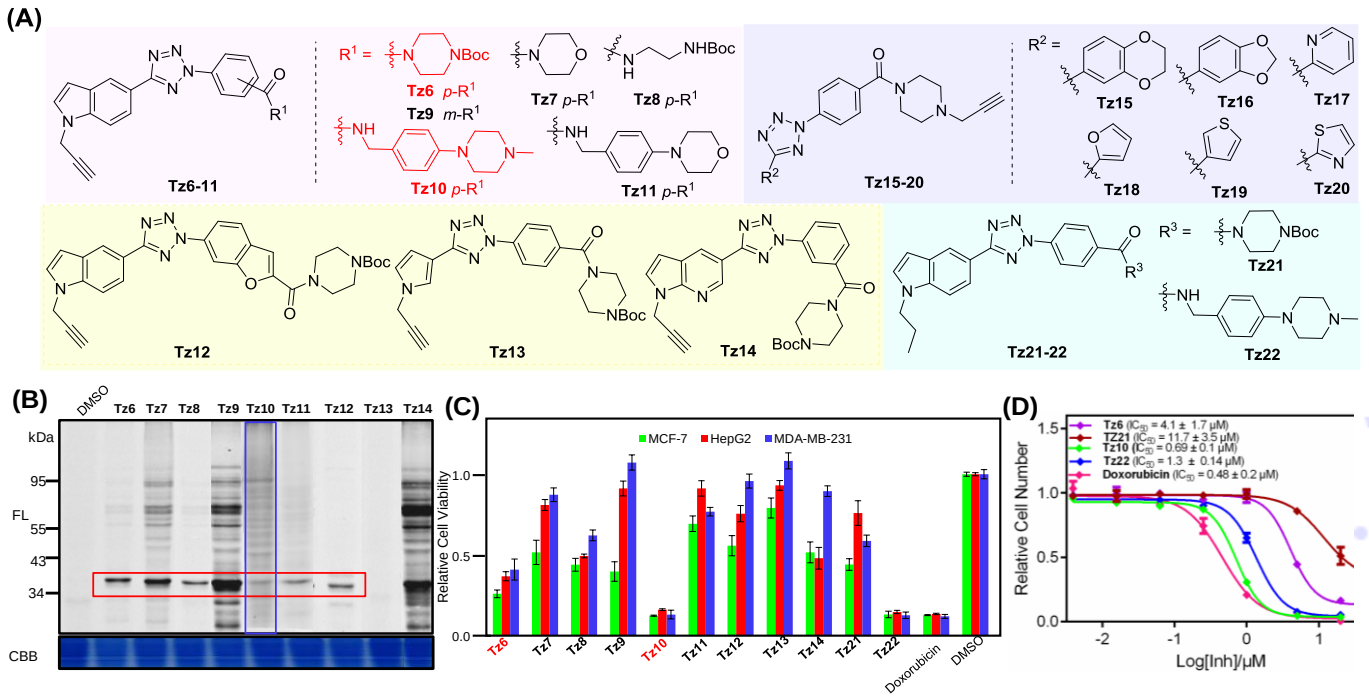


***Figure 2.*** (A) Stuctures of the probes **Tz6-22** (red-coloured probes were used in the following biological studies). (B) Proteome reactiv profiles of live MCF-7 cells treated with **Tz6-14** (5 μM final concentration, 10 min of UV irradiation). (C) Inhibition of cancer cell viabil of **Tz6-22** determined by CCK8 assay. (D) $IC_{50}$ values of **Tz6/10/21/22** against MCF-7 cells.

strategies, we endeavored to incorporate a diaryltetrazole, a group can simultaneously act as a photo-crosslinker and a bioactive moiety, and an alkyne handle into a 20-membered small molecule library, with the aim to discover bioactive tetrazole-based molecules followed by identifying the interacting cellular targets.

Given that the effects of different substituents on the photolysis of tetrazole have not been well studied, we synthesized five probes (**Tz1-5**) bearing methyl, ester, phenyl, 2-pyridyl and 2-pyrimidyl groups, respectively, at the 5- position, following the typical synthetic methods of tetrazoles (Figure 1B, and Schemes S1 & S2);[14] an alkyne handle was embedded into the probes for visualization, enrichment, and identification of interacting proteins. We first evaluated the rate of photolysis of **Tz1-5** by HPLC analysis (Figure S1); upon exposure of each of the probes (dissolved in PBS buffer) to 302 nm UV light for different periods of time followed by HPLC separation of the reaction products, complete photolysis of **Tz1** and **Tz2** was observed within 5 and 2 min, respectively, indicating that the electron-withdrawing ester group in **Tz2** was beneficial for the photolysis. Interestingly, **Tz3/4/5** appeared to be more efficient than **Tz1/2** and their complete photolysis could be observed in as little as 1 min. Next, time-dependent labeling with bovine serum albumin (BSA) was carried out to assess the photo-crosslinking ability of these probes. Upon incubation of BSA with each of the probes for 10 min in PBS buffer, the resulting mixtures were exposed to UV light (302 nm) for different periods of time, clicked with TAMRA-$N_3$ and separated by SDS-PAGE. Fluorescently labeled BSA was finally visualized and quantified by in-gel fluorescence scanning (Figure 1C); we observed strong fluorescent bands of **Tz4**/BSA labeling in as little as 20 s with 1 μM of the probe. On the contrary, the labeling profiles of **Tz1/2/3/5** appeared to be significantly weaker under the same labeling conditions across all UV irradiation time. Further, we carried out labeling profiles of MCF-7 lysates with **Tz1-5** under the same labeling conditions as BSA labeling, which also appeared that only **Tz4**-treated sample showed notable labeling bands (Figure 1D, lan 4). These results indicate that 2,5-diphenyltetrazole (**Tz4**) is a efficient photo-crosslinker with superior protein crosslinking ability Encouraged by the excellent *in vitro* cross-linking efficiency of **Tz4** we sought to assess its *in situ* labeling properties. Upon incubatio of **Tz1-5** with live MCF-7 cells for 5 h, the cells were irradiate with UV light and then lysed; the resulting cell lysates wer conjugated with TAMRA-$N_3$, separated by SDS-PAGE followed b in-gel fluorescence scanning (Figure 1E); only **Tz4**-treated sample gave fluorescently labeled bands, highlighting the efficient labelin ability of 2,5-diphenyltetrazole *in situ*. To identify the crosslinke targets in cell lysates and live cells, labeled proteins under bot settings were clicked with TAMRA-Biotin-$N_3$ and then enriche using avidin-agarose beads, separated on SDS-PAGE, followed b LC-MS/MS analysis. As listed in Table S1, a series of high abundance proteins, such as CD9, CD44, PRC1 and CC2D1A, wer positively identified. Compared with previously reporte background inventory of three common photocrosslinkers (diazirine benzophenone and arylazide),[8] the background proteins c diaryltetrazole include unique and common proteins, which can b useful references for A*f*BP, especially in cases where diaryltetrazol is chosen as a photocrosslinker in the probe design.

After confirming that 2,5-diphenyltetrazole is an efficient photc crosslinker under both *in vitro* and *in situ* settings, we next set out t prepare a photoprobe library by incorporating different substituents at the 2- and 5- positions (**Tz6-20**, Figure 2A). The synthesis was largely based on published methods (Scheme S3-6). Two nonclickable analogues of **Tz6** and **Tz10**, **Tz21** and **Tz22,** were prepared accordingly as competitors (Scheme S7). With these probes in hand, we first evaluated the labeling performance of the library in mammalian cells (5 μM final probe concentration, 10 min of UV irradiation). As shown in Figure 2B, individual probes showed markedly distinct protein labeling profiles, which indicates the diversity elements introduced into the probe library were

10.1002/anie.201709584

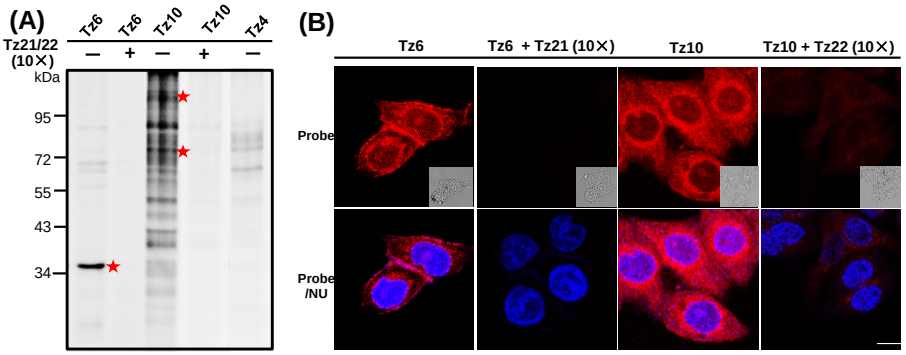


(C)

| Gene name | MW/ kDa | LFQ intensity ratio | | | | |
|---|---|---|---|---|---|---|
| | | Tz6/ (Tz6 + 10× Tz21) | Tz6/ Tz4 | Tz10/ (Tz10 + 10× Tz22) | Tz10/ Tz4 | Tz10/ Tz11 |
| ANXA2 | 38 | ∞ | ∞ | 0 | 0 | 0 |
| CKAP4 | 66 | 2.5 | ∞ | 0 | 0 | 0 |
| PDIA4 | 72.9 | ∞ | ∞ | 0 | 0 | 0 |
| NOS2 | 131 | 0 | 0 | ∞ | ∞ | ∞ |
| FLAD1 | 65 | 0 | 0 | ∞ | ∞ | ∞ |
| MRC2 | 166 | 0 | 0 | ∞ | ∞ | 5.1 |
| TPP1 | 60.4 | 0 | 0 | 2.6 | ∞ | ∞ |
| MLEC | 32.2 | 0 | 0 | 2.7 | ∞ | ∞ |

(D)

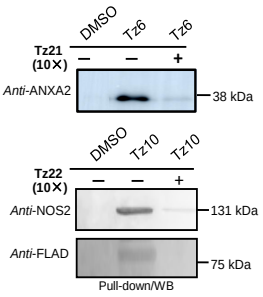


***Figure 3.*** (A) Proteome reactivity profiles of live MCF-7 cells treated with **Tz4/6/10** in the presence or absence of corresponding competitors (2 μM final concentration, 10 min of UV irradiation). (B) Live cell imaging of MCF-7 cells with **Tz6/10** (2 μM) in the presence or absence of corresponding competitors. Sacle bar = 10 μm. (C) High-confidence protein hits of **Tz6/10**, "∞" means infinity, "0" means not appearing. (D) Validation of three protein hits by pull-down/WB**.** WB = Western blotting.

sufficient to direct preferential bindings of different probes to various sub-proteomes in the cells. Interestingly, these *in situ* proteome reactivity profiles were different from the corresponding profiles obtained under *in vitro* conditions (Figure S3A), indicating that the probes interacted with different sets of proteins between live cells and cell lysates.

Subsequently, we tested the inhibitory activities of the probe library against three common cancer cell lines (MCF-7, HepG2 and MDA-MB-231; Figures 2C/D & S2). Gratifyingly, two probes, **Tz6** and **Tz10**, exhibited potent antiproliferative effects under normal cell culture conditions with $IC_{50}$ values of 4.1 and 0.69 μM, respectively. Remarkably, the cytotoxicity of **Tz10** was comparable to doxorubicin (a well-known anticancer drug). The corresponding alkyne handle-free competitors, **Tz21/22**, displayed comparable antiproliferative activities in MCF-7 cells (Figure 2C/D). We found that the structures of **Tz6/10** differ from the other molecules only in the amide moiety, suggesting that this part is essential for maintaining the compounds' observed bioactivities. Similar to previously reported bioactive molecules,[13a] probes bearing a *t*-butoxycarbamoylpiperazine carbonyl group (i.e. **Tz6/9/14**) also exhibited moderate antiproliferative effects in MCF-7 cells (Figure 2C).

To identify the cellular targets of the two most potent probes, **Tz6/10**, chemoproteomic experiments and live-cell bioimaging were next carried out concurrently. As shown in Figure 3A, the *in situ* proteome labeling was performed by following the procedures described above with the inactive **Tz4** probe as a control (lane 5), but at a lower probe concentration (2 μM) in order to reduce nonspecific binding. As shown in Figure 3A, while the **Tz4**-treated sample showed an overall negligible, nonspecific labeling profile (lane 5), which again confirmed the low background labeling property of tetrazole photo-crosslinkers in general as earlier discussed (e.g. Figure 1), the **Tz6**-treated sample showed a highly selective probe labeling profile, with a strong fluorescently labeled band predominantly at ~37 kDa and several much fainter bands at ~72 kDa (lane 1), indicating excellent target selectivity. In the presence of excessive **Tz21** (10 x) as a competitor, all fluorescent bands including the 37-kDa band were abolished (lane 2), indicating they were potential **Tz21**-targeted proteins and not background proteins caused by nonspecific photo-crosslinking. In shar contrast, the **Tz10**-treated sample showed significantly less selective, albeit still **Tz22** competitive, probe labeling profiles, resultin in strong fluorescently labeled band throughout the whole lane (lane 3). To trac the subcellular probe localization, cellula imaging of live MCF-7 cells with **Tz6/10** wa next carried out. The cells were first treate with each probe followed by UV irradiation t initiate photo-crosslinking. Subsequently cells were fixed, permeabilized and clicke with TAMRA-$N_3$ under previously optimize click chemistry conditions,[5b,5c,9] then imaged Strong fluorescence signals were observed i the cell membrane and nucleus from **Tz6** treated cells, while **Tz10** mainly located outside of the nucleus Consistently, the fluorescence signals of both probes were abolishe in the presence of excessive competitors (Figure 3B). Contro imaging experiments with DMSO under similar conditions gav minimal background fluorescence compared to labeled cells (Figur S5). Results from these competitive in situ labeling and live-ce imaging experiments thus indicate that both **Tz6** and **T10** were abl to efficiently capture their intended cellular targets, and **Tz** appeared to have highly selective cellular targets.

We next proceeded to identify potential cellular targets of **Tz6/1** by large-scale chemoproteomics experiments. Similar to th procedures described above, probe-labeled proteins were affinity purified and identified by LC-MS/MS analysis following *in sit* proteome labeling and click chemistry with TAMAR-Biotin-N Control experiments were done concurrently with DMSO- and **Tz4** treated control samples, which served to filter off "false hits identified from the LC-MS/MS experiments as a result c background photo-crosslinking and/or nonspecific protein binding In addition, only proteins that appeared in duplicated runs an whose LFQ intensity[15] ratios from probe-treated and competitive labeling experiments (i.e. **Tz6** *vs* (**Tz6** + 10× **Tz21**), or **Tz10** *vs* (**Tz10** + 10× **Tz22**) of greater than 2 were considered further. Finally, a comparison of the proteomic targets of **Tz10** versus **Tz11**, an inactive analogue differs only in the position of piperidine, was made to reveal proteins relevant for antiproliferative activity of **Tz10** (LFQ ratio > 2). As listed in Figure 3C and Table S3/4, 35 and 60 protein hits met these criteria for **Tz6** and **Tz10**, respectively. Further analysis of these protein hits revealed that annexin A2 (ANXA2) could match the ~37-kDa major band detected in **Tz6**-labeled proteomes (i.e. Figure 3A, * in lane 1), while flavin adenine

dinucleotide synthetase 1 (FLAD1) and nitric oxide synthase (NOS2) could match the labeling bands at ~70 kDa and ~130 kDa, respectively, in **Tz10**-treated sample (Figure 3A, * in lane 3). These three target candidates were further validated by pull-down/Western blotting (WB) with the corresponding antibodies (Figure 3D). Moreover, we found that the locations of most proteins hits coincided well with the imaging results (Figure 3B);[16] for example, the protein hits of **Tz6**, ANXA2, VDAC and CKAP4, are known to be mainly located in the cell membrane, and NOS2, FLAD1 of **Tz10**-identified proteins are predominantly cytosolic proteins. We further verified ANXA2 and NOS2 by the immunofluorescence experiments, following our previous protocols (Figure S5).[5b,5c] These lines of evidence underscored the high reliability of these protein hits, and it is possible that **Tz6/10** produce their antiproliferative effects through a combination of these protein targets.

Considering annexin A2 is a cancer biomarker,[17] it is of great importance to develop suitable small molecule probes that can detect its cellular expression/activity *in situ*. Herein, we further evaluated the labeling sensitivity of **Tz6** and other probes toward annexin A2 by concentration- and time-dependent labeling experiments. As shown in Figure 4A, **Tz6/8/12** can successfully label ANXA2 at 2 μM probe concentration, which was confirmed by pull-down/WB (Figure 4A, bottom gel). An even lower concentration of the probes (1 μM) was sufficient to produce prominent corresponding bands in live MCF-7 cells from concentration-dependent labeling experiments (Figure S3C, SI). Time-dependent labeling experiments revealed that the ~37 kDa band was visible within 1 h (Figure 4B). Importantly with **Tz6**, the highly selective ANXA2 labeling profiles could be successfully recapitulated in various cancer cell lines, including HepG2, A549, HeLa and MDA-MB-231 (Figure 4C), suggesting that this probe has the potential of broad applications in detecting endogenous ANXA2. It is also noteworthy that, from the immunofluorescence (IF) experiments performed with anti-ANXA2, the resulting fluorescence signals appeared to overlap well with those obtained from staining the same cells with **Tz6** (Figures 4D & S5), implying that **Tz6** can report this protein's activities by both protein labeling and live-cell imaging experiments. In addition, labeling experiments of recombinant annexin A2 with **Tz6** revealed that the protein could be successfully labeled by the probe at as low as 0.5 μM probe concentration with 1 μg of the protein, and as little as 1.25 pmol of the protein could be successfully detected by **Tz6** at 1 μM concentration (Figure 4E), proving that this probe possesses excellent sensitivity toward annexin A2. To map the potential labeling sites of **Tz6** in annexin A2, the probe-labeled recombinant protein was analyzed by LC-MS/MS. $Asp^{110}$, a residue located in the active region of the protein was positively identified (Figures 4F & S6).[18] This crosslinking pattern is consistent with the results previously reported by us and others.[9,12] Docking experiments revealed that the distance between the tetrazole in **Tz6** and $Asp^{110}$ was around 7.7 Å, which is a reasonable distance for successful photo-crosslinking. Finally, we evaluated the photo-crosslinking efficiency of **Tz6** with recombinant annexin A2 by pull-down/WB, which appeared to be very high (Figure S7).

In conclusion, we demonstrated that 2,5-diphenyltetrazole can display superior photo-crosslinking efficiency under both *in vitro* and *in situ* settings. Diaryltetrazole-based probes bearing an alkyne handle were suitable for integrated phenotypic screening and target identification. We identified the cellular targets of two hit

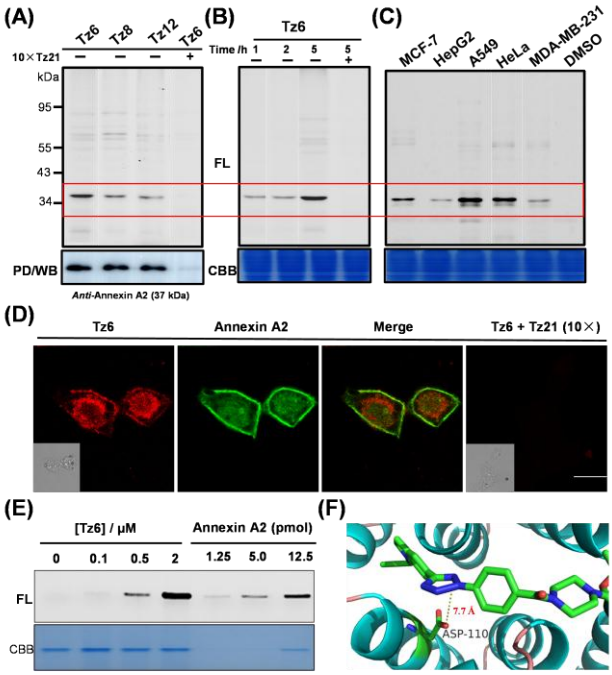


Figure 4. (A) Labeling profiles of MCF-7 cells with **Tz6/8/12** ( μM), in the presence or absence of competitor (**Tz21**). Th corresponding pull-down/Western blot (WB) are shown (botto gel). (B) Time-dependent *in situ* labeling with **Tz6** (2 μM). (C Labeling profiles of different cancer cell lines with **Tz6** (2 μM (D) Live-cell imaging of MCF-7 cells with **Tz6** (2 μM Immunofluorescence (IF) staining using *anti*-annexin A antibodies. Sacle bar = 10 μm. (E) Labeling of recombina annexin A2 protein with **Tz6** (different concentrations of **Tz6** ( different amount of protein). (F) ASP-110, the binding site of **Tz** with annexin A2 identified by LC-MS/MS and dockin experiments to predict the binding mode of **Tz6** with annexin A2.

compounds, **Tz6/10**, by affinity-based proteome profiling couple with live-cell bioimaging. Most protein hits are disease-relate targets. Importantly, several probes from our current study especially **Tz6**, were able to label endogenous annexin A2 wit excellent selectivity and sensitivity under highly complex nativ cellular environments from different mammalian cells. With thes outstanding properties, we expect that these novel small molecul probes could find potential applications in cancer-related diagnose and therapy.

**Keywords:** tetrazole · phenotypic screening · target identification. affinity-based probe · cancer biomarker

[1] a) J. G. Moffat, J. Rudolph, D. Bailey. *Nat. Rev. Drug Disco* **2014**, *13*, 588-602. b) S. J. Warchal, A. Unciti-Broceta, N. C Carragher. *Future Med. Chem.* **2016**, *8*, 1331-1347.

[2] E. Dominguez, A. Galmozzi, J. W. Chang, K. L. Hsu, J. Pawlak W. Li, C. Godio, J. Thomas, D. Partida, S. Niessen, P. E O'Brien, A. P. Russell, M. J. Watt, D. K. Nomura, B. F. Cravatt, E. Saez. *Nat. Chem. Biol*. **2014**, *10*, 113-121.

[3] a) T. Anastassiadis , S.W. Deacon, K. Devarajan, H. Ma and J. R. Peterson. *Nat. Biotechnol.* **2011**, *29*, 1039-1045. b) M. Bantscheff , D. Eberhard , Y. Abraham , S. Bastuck , etc. *Nat. Biotechnol*. **2007**, *25*, 1035-1044.

[4] S. Pan, H. Zhang, C. Wang , S. C. Yao, S. Q. Yao, *Nat. Prod. Rep*. **2016**, *4*, 612-620. b) J. Sumranjit, S. J. Chung, *Molecules* **2013**, *18*, 10425-10451.

[5] a) H. Guo, Z. Li, *Med. Chem. Comm*. **2017**, *8*, 1585-1591. b) Z. Li,; P. Hao, L. Li, C. Y. J. Tan, X. Cheng, G.Y. J. Chen, S. K.

10.1002/anie.201709584

Sze, H.-M. Shen, S. Q. Yao, *Angew. Chem. Int. Ed*. **2013**, *52*, 8551-8556; c) Z. Li, D. Wang, L. Li, S. Pan, Z. Na, C. Y. J. Tan, S. Q. Yao, *J. Am. Chem. Soc.* **2014**, *136*, 9990-9998

[6] E. Smith, I. Collins, *Future Med. Chem.* **2015**, *7*, 159–183.

[7] H. Guo, J. Xu, P. Hao, K. Ding, Z. Li, *Chem. Commun*. **2017**, *53*, 9620-9623.

[8] a) J. Park, M. Koh, J. Y. Koo, S. Lee and S. B. Park, *ACS Chem. Biol*. **2016**, *11*, 44–52. b) H. Park, J. Y. Koo, Y. V. Srikanth, S. Oh, J. Lee, J. Park, S. B. Park, *Chem. Commun*. **2016**, *52*, 5828-5831. c) P. Kleiner, W. Heydenreuter, M. Stahl, V. S. Korotkov and S. A. Sieber, *Angew. Chem., Int. Ed*. **2017**, *56*, 1396–1401.

[9] Z. Li, L. Qian, L. Li, J. C. Bernhammer, H. V. Huynh, J. S. Lee and S. Q. Yao, *Angew. Chem. Int. Ed*. **2016**, *55*, 2002-2006.

[10] S. Yoshikawa, T. Tanimura, A. Miyawaki, M. Nakamura, M. Yuzaki, T. Furuichi, K. Mikoshiba, *J. Biol. Chem.* **1992**, *267*, 16613-16619.

[11] L. Leder, *Methods Mol. Biol*. **2015**, *1266*, 7-27.

[12] A. Herner, J. Marjanovic, T. M. Lewandowski, V. Marin, M. Patterson, L. Miesbauer, D. Ready, J. Williams, A. Vasudevan, Q. Lin, *J. Am. Chem. Soc.* **2016**, *138*, 14609−14615.

[13] a) J. S. Cisar, B. F. Cravatt, *J. Am. Chem. Soc.***2012**, *134*, 10385-10388. b) T. Kambe, B. E. Correia, M. J. Niphakis, B. F. Cravatt, *J. Am. Chem. Soc.* **2014**, *136*, 10777-10782. c) C. G. Parker, A. Galmozzi, Y. Wang, B. E. Correia, K. Sasaki, C. M. Joslyn, A. S. Kim, C. L. Cavallaro, R. M. Lawrence, S. R. Johnson, I. Narvaiza, E. Saez, B. F. Cravatt. *Cell* **2017**, *168*, 527-541.

[14] Y. Wang, W. Song, W. J. Hu, Q. Lin, *Angew. Chem. Int. Ed.* **2009**, *48*, 5330–5333.

[15] J. Cox, M. Y. Hein, C. A. Luber, I. Paron, N. Nagaraj, M. Mann. *Mol. Cell Proteomics*. **2014**, *13*, 2513-26.

[16] The information about the protein locations were obtained from Genecards database (http://www.genecards.org/).

[17] a) F. Tas, C. Tilgen Yasasever, S. Karabulut, D. Tastekin, D. Duranyildiz. *Biomed. Pharmacother.* **2015**, *69*, 237-241. b) Y. R. Jeon, S. Y. Kim, E. J. Lee, Y. N. Kim, D. Y. Noh, S. Y. Park, A. Moon, *Proteomics* **2013**, *13*, 3145-3156.

[18] Y. Liu, H. K. Myrvang, L. V. Dekker. *Br. J. Pharmacol*. **2015**, *172*, 1664-1676.

10.1002/anie.201709584

*Target identification*

# Tetrazole-Based Probes for Integrated Phenotypic Screening, Affinity-based Proteome Profiling and Sensitive Detection of a Cancer Biomarker

K. Cheng, J.-S. Lee, S. Q. Yao, K. Ding,* Z. Li, * __ **Page – Page**

**Entry for the Table of Contents** (Please choose one layout)

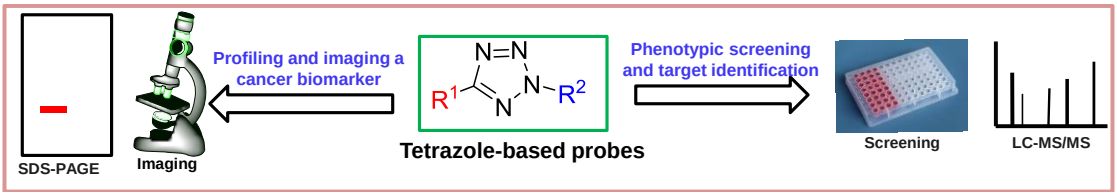


Tetrazole-based probes bearing an alkyne handle are suitable for phenotypic screening and affinity-based proteome profiling especially **Tz6** that can sensitively detect a cancer biomarker by both protein labeling and bioimaging.